SOFT ROBOTS

Bioinspired living structural color hydrogels

Fanfan Fu, Luoran Shang, Zhuoyue Chen, Yunru Yu, Yuanjin Zhao*

Structural color materials from existing natural organisms have been widely studied to enable artificial manufacture. Variable iridescence has attracted particular interest because of the displays of various brilliant examples. Existing synthetic, variable, structural color materials require external stimuli to provide changing displays, despite autonomous regulation being widespread among natural organisms, and therefore suffer from inherent limitations. Inspired by the structural color regulation mechanism of chameleons, we present a conceptually different structural color material that has autonomic regulation capability by assembling engineered cardiomyocyte tissues on synthetic inverse opal hydrogel films. The cell elongation and contraction in the beating processes of the cardiomyocytes caused the inverse opal structure of the substrate film to follow the same cycle of volume or morphology changes. This was observed as the synchronous shifting of its photonic band gap and structural colors. Such biohybrid structural color hydrogels can be used to construct a variety of living materials, such as two-dimensional self-regulating structural color patterns and three-dimensional dynamic *Morpho* butterflies. These examples indicated that the stratagem could provide an intrinsic color-sensing feedback to modify the system behavior/action for future biohybrid robots. In addition, by integrating the biohybrid structural color hydrogels into microfluidics, we developed a "heart-on-a-chip" platform featuring microphysiological visuality for biological research and drug screening. This biohybrid, living, structural color hydrogel may be widely used in the design of a variety of intelligent actuators and soft robotic devices.

INTRODUCTION

Structural colors, originating from the physical interaction of light with intrinsic periodic nanostructures, have been widely observed and intensively investigated in a range of living microorganisms, flora, and fauna (*1*–*7*). Inspired by these natural examples, many elaborately nanostructured photonic materials with brilliant structural colors have been developed by using various inorganic, polymeric, and other hybrid components (*8*–*17*). Such bioinspired structural color materials can strongly modulate electromagnetic waves and manipulate the propagation of photons with the energy in their photonic band gap (PBG) (*8*, *9*). In particular, if a structural color material is made from a hydrogel polymer, the swelling or shrinking after stimulation of the polymer leads to a change in the PBG and therefore the structural color (*18*–*21*). This feature enables structural color hydrogels to offer technological advances, such as in switch construction, optical displays, sensing materials, anti-counterfeiting labels, intelligent skins, and wearable electronics (*22*–*30*). However, unlike some natural creatures that can autonomously regulate their structural colors, current bioinspired, responsive, structural color materials all require external stimuli to display their functionality. This leads to complex systems and limits their further applications. Therefore, the development of bioinspired structural color materials that have an autonomic regulation capability will be of value in the construction of next-generation intelligent photonic devices.

Inspired by the structural color shift mechanism of chameleons (*31*), which occurs through the control of dermal iridophores via active tuning of their guanine nanocrystal lattice PBGs (Fig. 1A), we describe structural color materials that have an autonomic regulation capability. These were produced by assembling engineered cardiomyocyte tissues on synthetic inverse opal hydrogel films (Fig. 1B). Taking advantage of the surface microgroove structure and high biocompatibility of the hydrogel, the assembled cardiomyocytes were able to recover their autonomic beating ability with guided cellular orientation and improved contraction performance on the elastic films. Because the cardiomyocytes' beating processes are accompanied by cell elongation and contraction, the substrate inverse opal hydrogel film on the substrate will undergo the same cycle of volume or morphology changes. This, in turn, appears as synchronous shifts in their PBGs and structural colors. On the basis of these biohybrid structural color hydrogels, a variety of living materials becomes possible, including two-dimensional (2D) self-regulating structural color patterns and 3D dynamic *Morpho* butterflies. These examples indicated that the stratagem could provide an intrinsic color-sensing feedback to modify the system behavior/action for future biohybrid robots. In addition, with the integration of biohybrid structural color hydrogels and microfluidics, we developed a heart-on-a-chip device featuring microphysiological visuals for biological research and drug screening. These examples demonstrate that biohybrid living structural color hydrogels are highly versatile devices capable of a wide variety of applications.

RESULTS

In a typical experiment, the inverse opal–structured color hydrogel films were fabricated by replicating silica colloidal crystal templates, as shown in Fig. 2A. First, these colloidal crystal templates were prepared by the self-assembly of silica nanoparticles (with sizes of 225, 250, 270, 295, and 300 nm) on the surface of glass slides or micropatterned silicon wafers, which became closely packed and formed an ordered colloidal crystal array structure during solvent evaporation (Fig. 2B). This ordered packing of the silica nanoparticles endowed the colloidal crystal arrays with interconnected nanopores throughout the templates, which facilitated the methacrylated gelatin (GelMA) pregel solution infiltration. Next, after the pregel solution had penetrated the nanopores and filled all voids in the colloidal crystal templates by capillary action, it was polymerized to form hydrogel hybrid colloidal crystal templates by ultraviolet (UV) light (Fig. 2C). Last, the free-standing inverse opal–structured hydrogel films with a thickness of about 150 μm were obtained by etching the silica nanoparticles of the hybrid templates (Fig. 2D and fig. S1A).

State Key Laboratory of Bioelectronics, School of Biological Science and Medical Engineering, Southeast University, Nanjing 210096, China.
*Corresponding author. Email: yjzhao@seu.edu.cn

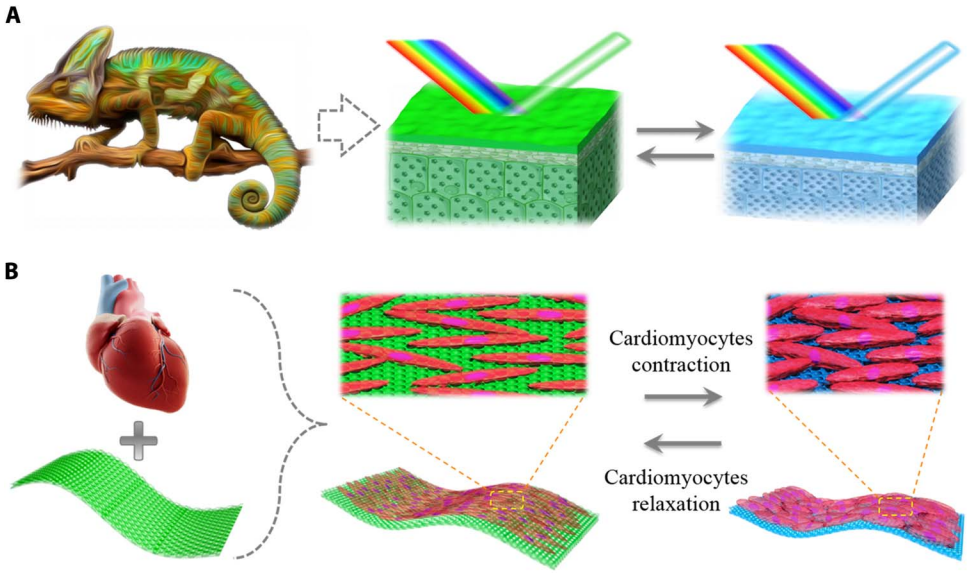

Fig. 1. Schemes of the structural color materials with autonomic regulation capability. (**A**) Structural color regulation mechanism of chameleons, which is achieved by controlling the dermal iridophores to actively tune their guanine nanocrystal lattice PBGs. (**B**) Schematic diagram of the construction of the bioinspired self-regulated structural color hydrogels by assembling engineered cardiomyocyte tissues on synthetic inverse opal hydrogel films.

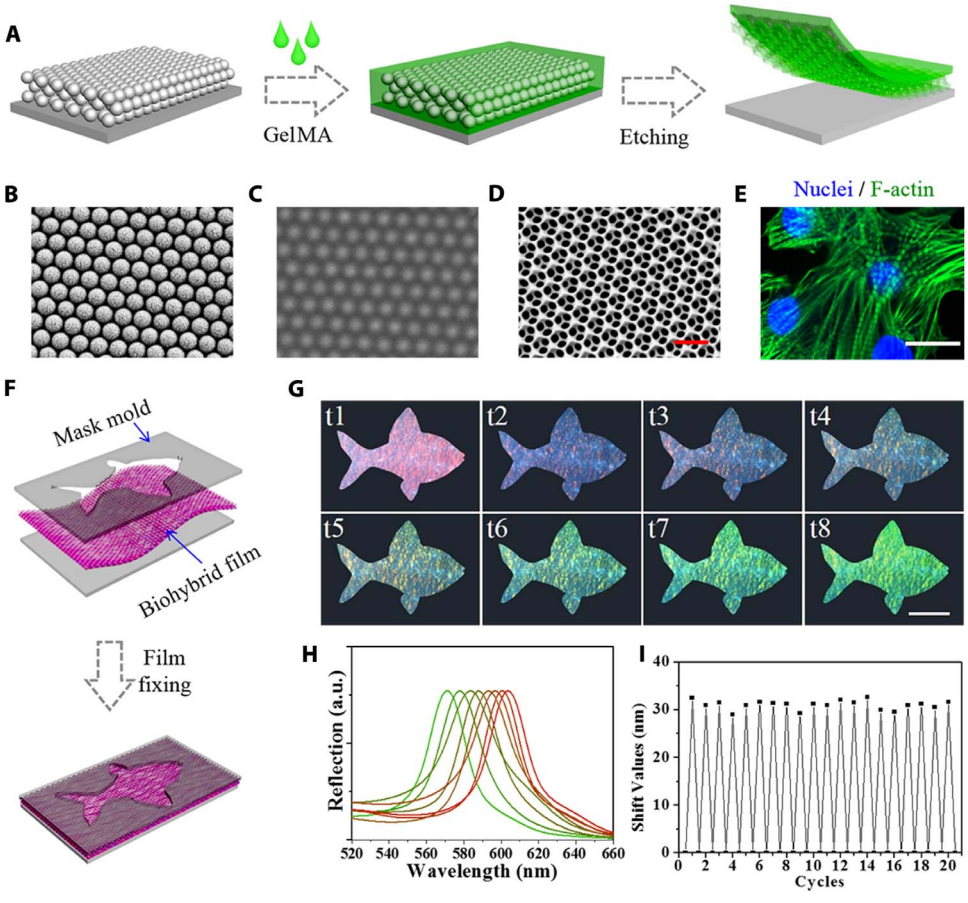

Fig. 2. Biohybrid structural color hydrogel films with autonomic iridescence displaying. (**A**) Schematic diagram of the generation process of the inverse opal–structured color hydrogel films. (**B** to **D**) SEM images of the colloidal crystal template, the hydrogel hybrid colloidal crystal, and the inverse opal–structured hydrogel film, respectively. (**E**) Fluorescent image of cardiomyocytes cultured on the surface of the structural color hydrogel film. (**F**) Schematic diagram of the fixed process of the biohybrid structural color hydrogel film. (**G**) Optical microscope images of the structural color variation process of the fixed biohybrid hydrogel film during one myocardial cycle. (**H**) Reflection spectra of the structural color hydrogel film in (G). The left-most (green) trace corresponds to t8 and the right-most red trace corresponds to t1. (**I**) Relationship between the reflection shift values of the biohybrid structural color hydrogel film and the 20 beating cycles of the cardiomyocytes on its surface. Scale bars, 500 nm (B to D), 20 μm (E), and 1 mm (G).

Because of the orderly arrangement of the structure of the silica colloidal crystal templates, the resultant inverse opal–structured hydrogel films were imparted with unique PBG properties. In particular, certain light wavelengths located in the PBG were prevented from propagating through the inverse opal structures and were reflected by the hydrogel film. Therefore, the inverse opal–structured hydrogel film displayed vivid structural colors and had characteristic reflection peaks (fig. S1B). The main characteristic reflection peak position of the hydrogel film

can be estimated by mathematical manipulation of the Bragg-Snell equation, that is

$$\lambda = 1.633D\left(n_{\text{average}}{}^2 - \cos^2\theta\right)^{1/2} \quad (1)$$

where D is the distance to the diffracting plane, n_{average} refers to the average refractive index of the inverse opal material, and θ is the Bragg glancing angle of incidence of the light falling on the nanostructures. Equation 1 implies that there are several approaches to regulating the structural colors of inverse opal hydrogel films, such as changing the diffracting plane spacing D or the Bragg glancing angle θ.

To mimic the structural color shift mechanism of chameleons and implement the concept of autonomic regulation of structural color materials, we used a bioactive GelMA as the pregel in the construction of the free-standing and flexible inverse opal–structured hydrogel films, which were used as substrates for neonatal rat ventricular cardiomyocytes (Fig. 2E and fig. S2). Because the GelMA hydrogel had modified extracellular matrix components (*32*–*34*), the resultant films were endowed with high biocompatibility and plasticity (figs. S3 and S4). This facilitated cardiomyocyte attachment and growth, promoted cellular alignment and elongation, and provided flexibility and the capacity for sustained cycles of expansion and contraction. The assembled cardiomyocytes recovered their stable autonomic beating after culturing for 2 days. The beating of the cardiomyocytes caused the inverse opal–structured GelMA hydrogel films to shrink or bend during systole (contraction) and return to their original shape due to the elasticity of the hydrogel films or the gravity of the hydrogel films during diastole (relaxation). These rhythmic volume or morphology changes in a hydrogel film corresponded to changes in its nanostructure, including the diffracting plane spacing and the Bragg glancing angle, both of which led to synchronous cycle shifts in the PBGs and structural colors. Therefore, this integration of engineered cardiomyocyte tissues and flexible inverse opal hydrogel films demonstrates the concept of biomimetic structural color materials with autonomic regulation capabilities. It points to potential creation of a variety of intelligent actuators and soft robotic devices.

Although the biohybrid structural color hydrogel films displayed autonomic iridescence, their colors shifted unevenly because of the irregular volume or morphology changes in the free-standing hydrogel films (first half of movie S1). To solve this problem, we used a mask mold with a fish-shaped pattern to immobilize the biohybrid free-standing hydrogel film in a fixed plane (Fig. 2F). In this case, irregular morphology changes in the structural color hydrogel film during the myocardial cycles were prevented, and the film could maintain a constant Bragg glancing angle (fig. S5A). In this way, the self-regulation of the hydrogel structural colors will be caused mainly by swelling- or shrinking-induced changes in the diffracting plane spacing, which should lead to a more uniform behavior. The resulting improvements were recorded by a high-speed color camera and analyzed by spectral software. It was observed that the structural color of the fish pattern hydrogel involved a blue shift from red to green that was periodic and uniform, as induced by the contraction and relaxation of the cardiomyocytes on the surface of the hydrogel film (Fig. 2G). During this process, the reflection peaks that read out a fixed vertical angle by using an optical microscope equipped with a fiber-optic spectrometer repeatedly shifted from 605 to 570 nm (Fig. 2H and second half of movie S1). The frequency of the structural color reflection peak regulation cycles corresponded to the beating frequency of the cardiomyocytes (Fig. 2I). For a flexible inverse opal material, there is a relationship between the

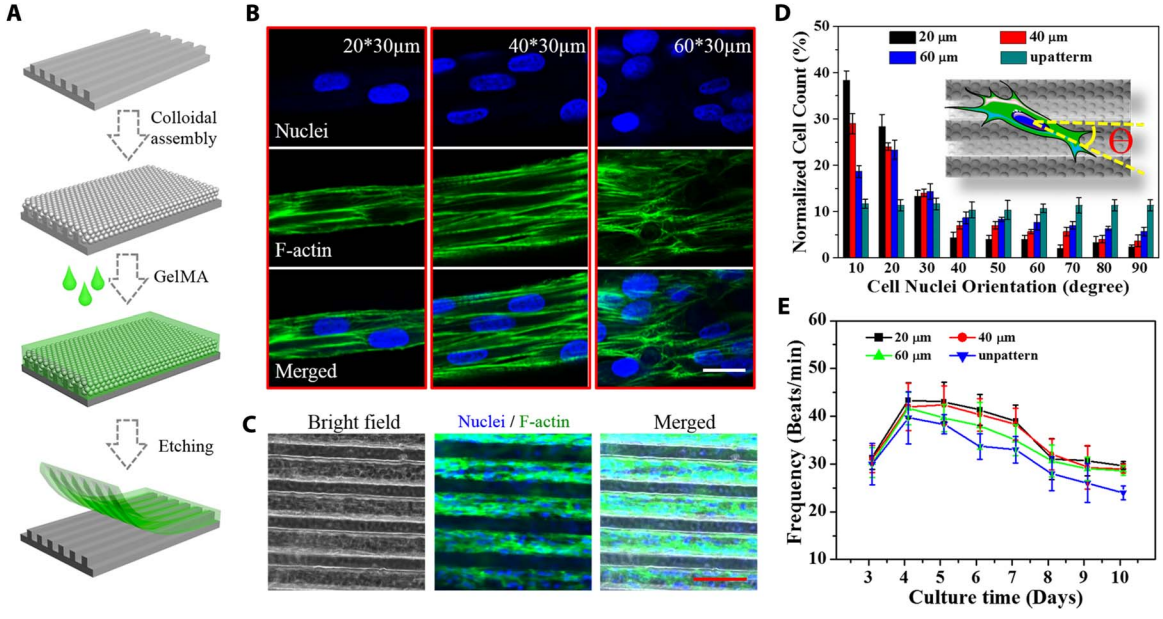

Fig. 3. Cardiomyocytes cultured on microgroove-patterned structural color hydrogel films. (**A**) Schematic diagram of the generation process of the microgroove-patterned hydrogel films. (**B**) Fluorescent images of the cardiomyocytes cultured on the surface of the structural color hydrogel films with different concave side and convex side values, from left to right, are 20 and 30 μm, 40 and 30 μm, and 60 and 30 μm, respectively. (**C**) Confocal laser scanning microscopy (CLSM) images of the anisotropic laminar cardiomyocyte tissues on the surface of the microgroove-patterned inverse opal–structured hydrogel film. (**D**) Orientation angle frequency distribution of the cardiomyocytes on differently patterned substrates after 6 days of culture. Error bars represent SD. (**E**) Beating characterization of the cardiomyocytes on different patterned substrate. These dates were the average values of each day (10 min each time and five times every day). Scale bars, 20 μm (B) and 100 μm (C).

subjected tension and the structural color changes (fig. S6). Therefore, the mechanical behavior and the contraction force of the assembled cardiomyocytes on the surface of the hydrogel film could be estimated, based on the degree of shift in the structural colors. This lays the foundation for the construction of biosensors that can modulate the contractile properties and stiffness of cells at nanoscale levels.

To further exploit the function of the biohybrid structural color hydrogel films, we designed the assembled cardiomyocytes on the film surfaces to be organized anisotropically, which we expected to mimic the conditions in an actual heart and therefore perform better during myocardial cycles. To achieve this, we used silicon wafers with microgroove patterns for the self-assembly of silica colloidal crystal templates and hydrogel film replication, as in the scheme in Fig. 3A. The resultant GelMA hydrogel films had the same inverse opal nanostructure and complementary microgrooves (figs. S7 and S8). With these specific structures, the cultured cardiomyocytes tended to be aligned and elongated on the surface of the film. Inverse opal hydrogel films with three different filament spacings for the microgrooves were investigated, with concave side and convex side values of 20 and 30 μm, 40 and 30 μm, and 60 and 30 μm, respectively. The cardiomyocytes responded in each case by showing nonrandom sarcomere alignment, as confirmed in the three respective columns of images in Fig. 3 (B and C). The imaging was achieved by using phalloidin/4′,6-diamidino-2-phenylindole (DAPI) for F-actin and nuclei staining. The angles between the growth direction of the cardiomyocytes and the circumferential direction were measured and analyzed (Fig. 3D). The results indicate that about 55% of the cardiomyocytes showed an orientation within 30° of parallel to the circumferential direction for the microgrooves with 60-μm filament spacing. This value increased with reduced filament spacing, being about 65 and 80% for filament spacings of 40 and 20 μm, respectively.

The spontaneous beating frequencies of cardiomyocytes seeded on the inverse opal hydrogel films with the different microgrooves were also recorded, as shown in Fig. 3E. Because of the biocompatibility of the GelMA hydrogel, the cardiomyocytes could quickly adhere, spread, and grow on the hydrogel surface. These cardiomyocytes on the microgroove GelMA hydrogel films displayed much stronger and more synchronous beating frequencies within 2 days, whereas they need 4 days to achieve synchronous contractions with unobvious strength on the simple GelMA hydrogel film. In addition, the beat frequencies of the cardiomyocytes on the microgroove hydrogel films declined by only about 30% over the culture period from day 4 to day 10, compared with a 40% decrease for the plane hydrogel films over the same culture period. Although the cellular orientation and the spontaneous beating frequency could be increased slightly by using a smaller filament spacing for the microgrooves, their fabrication is much more complex, and high-quality inverse opal scaffold replication is difficult. Therefore, inverse opal–structured microgroove hydrogel films with an optimized filament spacing (convex side, 30 μm; concave side, 40 μm) were used for the subsequent experiments. For such a microgroove hydrogel film, the cardiomyocytes formed anisotropic laminar tissues (fig. S9) and regulated the structural colors of the film with a wide range of wavelengths (from 605 to 562 nm, detected from a fixed vertical angle to the film) and at a rapid response rate (movie S2 and fig. S10).

Biohybrid structural color hydrogels have many attributes that make them an excellent choice for applications in soft robotics. As a demonstration, an inverse opal–structured GelMA hydrogel film with a butterfly morphology and radial microgrooves was designed and constructed

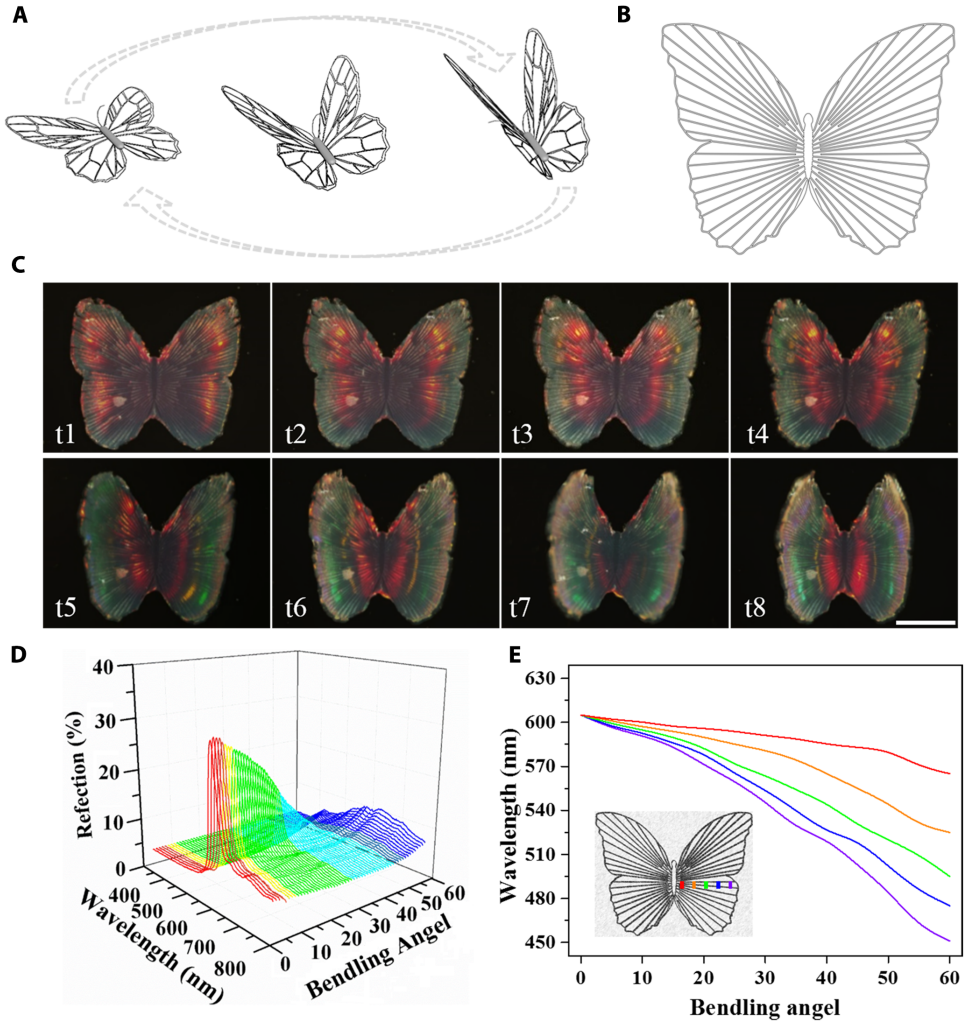

Fig. 4. The construction of soft structural color robotics by using the biohybrid hydrogels. (**A**) Schematic of a butterfly morphology hydrogel-generating thrust during the power of myocardial beating. (**B**) Schematic image of the butterfly skeleton with radial microgrooves. (**C**) Optical microscope images of the structural color variation process of the butterfly morphology structural color hydrogel during one myocardial cycle. Scale bar, 2 mm. (**D**) Dynamic reflectance wavelengths of the biohybrid hydrogel during one myocardial cycle at the position of the wing's outer edge. (**E**) Relationship between the bending angles of the biohybrid butterfly and the characteristic reflection peak values in different positions from the bionic butterfly center.

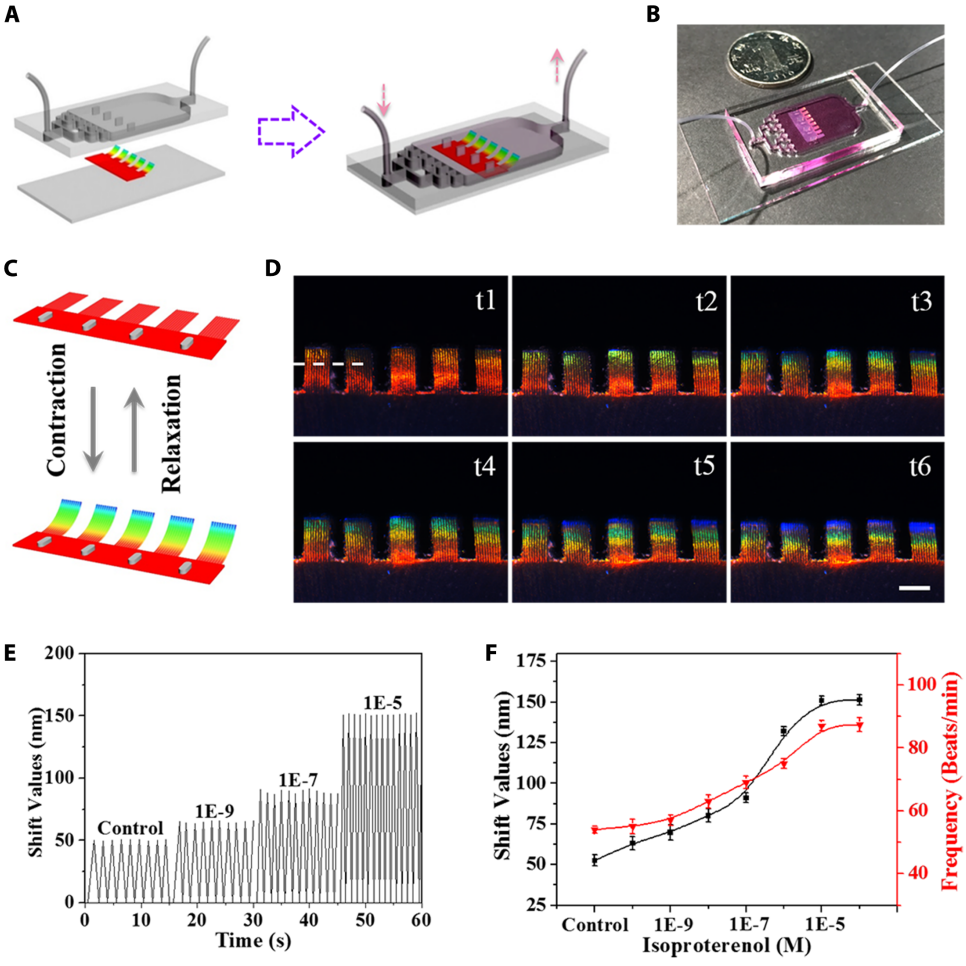

Fig. 5. The applications of the biohybrid structural color hydrogels in a heart-on-a-chip system. (**A**) Schematic of the construction of the heart-on-a-chip by integrating the biohybrid structural color hydrogel into a bifurcated microfluidic system. (**B**) Image of the biohybrid structural color hydrogel integrated heart-on-a-chip. (**C**) Schematic of the bent-up process of the biohybrid structural color hydrogels in heart-on-a-chip. (**D**) Dynamically optical microscope images of biohybrid structural color hydrogels during one myocardial cycle in a heart-on-a-chip system. Scale bar, 1 mm. (**E**) Relationship between the reflection peak shift values and the beating velocity of the biohybrid structural color hydrogels treated with different concentrations of isoproterenol at the position noted with dotted line in (D) (distance from the bottom/the total parallel microgroove-patterned hydrogel, 2/3). (**F**) Relationships of the average peak shift values (left) and the beating frequency (right) to the bent-up process of the biohybrid structural color hydrogels treated with different concentrations of isoproterenol. Error bars represent SD.

for cardiomyocyte assembly (Fig. 4, A and B). The cardiomyocytes formed an anisotropic laminar organization in the direction of the microgrooves and provided corresponding anisotropic and synchronous contractions and relaxations to the substrate. As a result, the butterfly morphology free-standing hydrogel film appeared to swing its wings with high-energy efficiency in the medium, like a real butterfly flying in air (movie S3). During this process, the structural color of the butterfly morphology free-standing hydrogel film was also changed reversibly from a fixed observation position (Fig. 4C). This can be ascribed mainly to the changes in the Bragg glancing angle, which is induced by the bending of the bionic butterfly wings (demonstrated in fig. S5B). At the same time as the bending occurred, the structural color red-to-green transition occurred first at the wing's outer edge and spread gradually to the inside of the wings. To investigate the relationship between the shifted structural colors and the bending angles, we used different positions from the bionic butterfly center to record the variations in the structural colors and characteristic reflection peak positions, as shown in Fig. 4 (D and E). For each position at different bending angles, the bionic butterfly therefore had a corresponding and specific structural color fingerprint, which could be valuable in the design of intelligent robotic actuators with self-reporting features. Many intelligent robotic actuators may be achieved if living structural color systems can integrate with optogenetic control strategies (*35*), which may also enable real-time closed-loop modulation of cardiomyocyte contraction.

To implement this concept, we integrated biohybrid structural color hydrogels with parallel microgrooves into a microfluidic system to form a heart-on-a-chip system (Fig. 5). Organ-on-a-chip systems, including the heart-on-a-chip system, are elaborate microengineered physiological devices that contain continuously perfused microfluidic chambers inhabited by living cells arranged to reproduce key features of specific human tissues and organs (*36*–*41*). This technology may bring benefits to biomedical areas, such as developing human in vitro models for healthy or diseased organs, enabling the investigation of fundamental mechanisms in disease etiology and organogenesis, benefiting drug development in toxicity screening and target discovery, and potentially serving as a replacement for animal testing (*35*–*38*, *42*–*47*). In this heart-on-a-chip system, the microfluidics involved bifurcated injection channels, thereby providing a uniform culture medium or a drug solution to the engineered cardiac muscle tissue on the biohybrid structural color hydrogel (Fig. 5, A and B). With its flexible characteristics and parallel microgroove structure, the semi-fixed biohybrid structural color hydrogel could be bended along the direction of the anisotropic organization of the laminar cardiomyocytes (Fig. 5C). This process was self-reported by the hydrogels via structural coloration and the reflection peak's blue shift, as caused by the decrease in the Bragg glancing angle (demonstrated in fig. S5B). Because the specific structural color or reflection peak fingerprint at each different position corresponded to the contraction force of the anisotropic laminar cardiomyocytes (demonstrated in Fig. 4, D and E), the integrated system could act as a functional platform for studying the cellular behavior of cardiomyocytes and their assembled tissues under different conditions.

To demonstrate the effectiveness of the heart-on-a-chip system, we pumped various concentrations of isoproterenol into the microfluidics and used to stimulate the cardiomyocytes. Under normal conditions, the structural colors at the annotated position of the biohybrid hydrogels changed from red to green (Fig. 5D and first half of movie S4), and their reflection peak was blue-shifted from 608 to 556 nm, whereas the colors

were changed to blue and peak positions shifted to 475 nm when 1 μM isoproterenol was added (second half of movie S4). With higher concentrations of isoproterenol, the degree of structural color changes and shift values for the reflection peaks of the biohybrid structural color hydrogels could be increased further (Fig. 5, E and F). The beat frequency of the cardiomyocytes was also regulated by the use of isoproterenol, showing a positive chronotropic response that matched the isoproterenol concentration (Fig. 5F). These results are consistent with the actual efficacy of isoproterenol in vivo, which can increase heart contractility and pump frequency. Therefore, a biohybrid structural color hydrogel can be used in a heart-on-a-chip system that acts as a biomimetic microphysiological platform for visualizable biological research and drug screening.

DISCUSSION

We developed structural color hydrogels that have autonomic regulation capability by assembling engineered cardiomyocyte tissues on soft inverse opal GelMA hydrogel films. Because of the high biocompatibility and the surface microgroove structures of the hydrogel, the assembled cardiomyocyte tissues could quickly recover their autonomic beating ability, with guided cellular orientation and improved contraction performance. During the autonomic beating process, the cardiomyocytes undergo cell elongation and contraction, with the inverse opal–structured hydrogel substrate exhibiting the same cycles of volume or morphology changes. These appear as synchronous changes in their PBGs and structural colors. On the basis of these biohybrid structural color hydrogels, we constructed 2D self-regulating structural color patterns and 3D dynamic *Morpho* butterflies. These examples demonstrate that biohybrid living structural color hydrogels are highly versatile options for the design of intelligent actuators and soft robotic devices.

The integration of the biohybrid living structural color hydrogels and microfluidics introduces a heart-on-a-chip technology with distinctive features. In contrast to other hydrogels and elastomer films, the biohybrid living inverse opal–structured hydrogels have the ability to self-report. Some cell behavior involving relatively weak cellular forces could easily be overlooked because these forces do not cause obvious morphological changes in the hydrogels or elastomer films. However, such weak cellular forces might be detectable as visible structural color changes or reflection spectra shifts on a biohybrid structural color hydrogel, because their inverse opal hydrogel scaffolds are more sensitive to cell behavior and can translate that behavior into visual signals. This not only makes possible testing different kinds of cardiomyocyte drugs, some of which could cause unobvious stimuli responses, but also provides a platform for studying the growth and differentiation of cells and revealing their biological essence, such as the evolution of induced pluripotent stem cells and other stem cells into cardiomyocytes. In addition, with further optimization of the biohybrid living structural color hydrogel, it may be possible to realize single cell–level detection via the heart-on-a-chip technology. We therefore conclude that biohybrid structural color hydrogels and their use in self-reporting heart-on-a-chip technology will play a profound role in the field of biomedical engineering.

MATERIALS AND METHODS

Materials

Five kinds of SiO_2 nanoparticles with sizes of 225, 250, 270, 295, and 300 nm were purchased from Nanjing Nanorainbow Biotechnology Co. Ltd. GelMA hydrogel was self-prepared. Gelatin (from porcine skin), methacrylic anhydride, pancreatin (form porcine pancreas), and trypsin were acquired from Sigma-Aldrich (St. Louis, MO). Dulbecco's modified Eagle's medium/nutrient mixture F-12 (DMEM/F-12), 1× Hanks' balanced salt solution (HBSS), and fetal bovine serum (FBS) were purchased from Life Technologies. Penicillin-streptomycin and isoproterenol were obtained from Gibco. 5-Bromo-2′-deoxyuridine (BrdU) was obtained from Sigma-Aldrich (St. Louis, MO). Cellulose dialysis membranes [molecular weight cutoff (MWCO), 8000 to 14,000] were acquired from Shanghai Yuanye Biotechnology Corporation (Shanghai, China). Collagenase type 2 was purchased from Worthington. Alexa Fluor 488 phalloidin and DAPI were obtained from Life Technologies. Water used in all experiments was purified using a Milli-Q Plus 185 water purification system (Millipore, Bedford, MA) with resistivity higher than 18 Mohm·cm.

Preparation of inverse opal GelMA hydrogel scaffold

These inverse opal GelMA hydrogel scaffolds were fabricated using a sacrificial template method. For the preparation of inverse structural color films, these colloidal crystal templates were first prepared with the self-assembly of silica nanoparticles on glass slides. Briefly, the SiO_2 nanoparticle solution [ethyl alcohol, 5 weight % (wt %)] with a variety of particle sizes self-assembled on glass slides by a vertical deposition method at invariant temperature and humidity for 3 days. During this process, the nanoparticles in the solution had a 100% diffusion rate to keep the concentration uniform. However, the diffusion of these deposited nanoparticles was stopped when they were assembled into ordered structures above the meniscus solid-liquid-air interface. Because the fabrication of the colloidal crystal templates was very mature, we could get the templates with high repeatability (more than 95%). Then, the glass with the SiO_2 nanostructures was calcined at 400°C for 4 hours to improve their mechanical strength, and the silica colloidal crystal templates were thus obtained. The GelMA pregel solution with a concentration of 0.15 g/ml was infiltrated into the silica colloidal crystal templates by capillary force, and then the pregel solution was exposed into UV light and polymerized to form a hybrid hydrogel. The diffusion of the silica nanoparticles from the colloidal crystal templates was not obvious. This could be confirmed from the scanning electron microscopy (SEM) images (Fig. 2, B and C), which showed same silica nanoparticles packing before and after the hydrogel infiltration. Last, the inverse opal GelMA hydrogel films were obtained by etching (2 wt % hydrofluoric acid) the silica nanoparticles of the hybrid hydrogel. For the preparation of patterned inverse structural color hydrogels, silicon wafers with microgroove patterns, such as varying channel sizes and spacings (30 × 20 μm, 30 × 40 μm, and 30 × 60 μm) or others patterns, were used for the self-assembly of silica colloidal crystal templates at the same condition. Then, the patterned inverse structural color hydrogel was obtained in the same way as the inverse structural color film preparation.

Isolation of neonatal cardiomyocytes

Cardiomyocytes were isolated from 1- to 2-day neonatal Sprague-Dawley rat pups, and these rat pups were supplied by the department of comparative medicine of Jinling Hospital (Nanjing, China). Briefly, the thorax of 1- to 2-day-old rat pups was opened, and the heart was surgically removed. Upon removing the atria, the hearts were cut into 0.5- to 1-mm^3 medium-sized pieces and placed in an HBSS (0.02% trypsin, 0.02% pancreatin, and 0.05% collagenase) for 12 min at 37°C with continuous gentle shaking three to five times. The solution composed mainly of cardiomyocytes and cardiac fibroblasts was collected into a DMEM/F-12 medium (20% FBS) solution. Subsequently, the solution

was filtered and centrifuged at 1250 rpm. Then, the cells were dispersed into a DMEM/F-12 solution (10% FBS and 0.1 mM BrdU) and preplated in a cell culture dish to enrich cardiomyocytes and cardiac fibroblasts. After 90 min, the unattached cells, which were essentially cardiomyocytes, were separated and cultured in the hydrogel materials with a definite cell concentration.

Cells cultured and image

Cardiomyocytes were regularly cultured and passaged with DMEM/F-12 medium supplemented with 10% FBS and 1% penicillin-streptomycin in a humidified incubator at 37°C with 5% CO_2. The structural color hydrogel samples were first disinfected by exposure to UV light for 5 hours and washed with sterile HBSS repeatedly before cell culture. Then, the obtained cardiomyocytes were seeded on the surface of hydrogel films and dispersed into a DMEM/F-12 solution (10% FBS, 1% penicillin-streptomycin, and 0.1 mM BrdU) for the first 3 days of culture. After this, the cardiomyocytes were continuously cultured and supplemented into the normal medium.

Thin films with cardiomyocytes were immunostained by day 6, and the procedures were implemented at room temperature. Samples were first fixed for 30 min in 4% (v/v) paraformaldehyde–phosphate-buffered saline (PBS) solution and then permeabilized with 0.3% (v/v) Triton X-100–PBS solution for 30 min. After permeabilization, samples were counterstained with Alexa Fluor 488 phalloidin (1:400 dilution) for F-actin staining. Subsequently, the nuclei were counterstained with a nuclei stain (DAPI) applied in PBS (1:1000 dilution). In between each step, the samples were washed with PBS at least three times. Confocal microscopy images were acquired using a Zeiss LSM700 laser scanning microscope (Zeiss, Heidenheim, Germany). To characterize the morphology of cardiomyocytes, we washed the samples repeatedly and dehydrated them with gradient ethanol (20, 40, 60, 80, and 100%) before SEM imaging.

Characterization

Reflection spectra were obtained at a fixed glancing angle, using an optical microscope equipped with a fiber-optic spectrometer (USB2000-FLG, Ocean Optics). SEM images of samples were taken by a scanning electron microscope (S-3000N, Hitachi). Confocal microscopy images were acquired using a Zeiss LSM700 laser scanning microscope (Zeiss, Heidenheim, Germany). Microscopy images of the samples were obtained with an optical microscope (BX51, Olympus) equipped with a charge-coupled device camera (Media Cybernetics Evolution MP5.0) and a digital camera (Canon 5D Mark II).

SUPPLEMENTARY MATERIALS

robotics.sciencemag.org/cgi/content/full/3/16/eaar8580/DC1

Fig. S1. The fabrication of the inverse opal–structured hydrogel films.

Fig. S2. SEM images of the surfaces of the biohybrid structural color hydrogel films with cardiomyocyte covering.

Fig. S3. Results of the cardiomyocyte 3-(4,5-dimethyl-2-thiazolyl)-2,5-diphenyl-2H-tetrazolium bromide (MTT) assays.

Fig. S4. The typical stress-strain (stress-stretch ratio) curves of the GelMA inverse opal structural color hydrogel.

Fig. S5. The schematic diagram of two different approaches for regulating the structural colors of the inverse opal hydrogel films.

Fig. S6. The relationships of the reflectance wavelength and the stretched intensity of the GelMA inverse opal structural color hydrogel films during the stretch.

Fig. S7. Optical images and reflection spectra of the five different kinds of the microgroove-patterned inverse opal–structured hydrogel films.

Fig. S8. SEM images of the microgroove-patterned inverse opal–structured hydrogel films.

Fig. S9. The 3D reconstruction CLSM images of the anisotropic laminar cardiomyocyte tissues.

Fig. S10. Shift of the reflection spectra of the structural colors films.

Movie S1. Optical images of a free-standing biohybrid structural color hydrogel (first half) and dynamic reflection spectra of the biohybrid structural color hydrogel fixed by mask mold (second half).

Movie S2. Optical images of a microgroove-patterned biohybrid structural color hydrogel.

Movie S3. Optical images of a robotic butterfly morphology structural color hydrogel flying in medium.

Movie S4. The bending process of a structural color heart-on-a-chip under normal medium (first half) and under isoproterenol stimulation (second half).

REFERENCES AND NOTES

1. A. R. Parker, H. E. Townley, Biomimetics of photonic nanostructures. *Nat. Nanotechnol.* **2**, 347–353 (2007).
2. P. Vukusic, Evolutionary photonics with a twist. *Science* **325**, 398–399 (2009).
3. P. V. Braun, Materials science: Colour without colourants. *Nature* **472**, 423–424 (2011).
4. L. Shang, Z. Gu, Y. Zhao, Structural color materials in evolution. *Mater. Today* **19**, 420–421 (2016).
5. Y. Zhao, Z. Xie, H. Gu, C. Zhu, Z. Gu, Bio-inspired variable structural color materials. *Chem. Soc. Rev.* **41**, 3297–3317 (2012).
6. M. X. Kuang, J. X. Wang, L. Jiang, Bio-inspired photonic crystals with superwettability. *Chem. Soc. Rev.* **45**, 6833–6854 (2016).
7. K. D. Gilroy, A. Ruditskiy, H.-C. Peng, D. Qin, Y. Xia, Bimetallic nanocrystals: Syntheses, properties, and applications. *Chem. Rev.* **116**, 10414–10472 (2016).
8. G. von Freymann, V. Kitaev, B. V. Lotsch, G. A. Ozin, Bottom-up assembly of photonic crystals. *Chem. Soc. Rev.* **42**, 2528–2554 (2013).
9. F. Gallego-Gómez, A. Blanco, C. López, Exploration and exploitation of water in colloidal crystals. *Adv. Mater.* **27**, 2686–2714 (2015).
10. M. Yang, H. Chan, G. Zhao, J. H. Bahng, P. Zhang, P. Král, N. A. Kotov, Self-assembly of nanoparticles into biomimetic capsid-like nanoshells. *Nat. Chem.* **9**, 287–294 (2017).
11. B. Bharti, A.-L. Fameau, M. Rubinstein, O. D. Velev, Nanocapillarity-mediated magnetic assembly of nanoparticles into ultraflexible filaments and reconfigurable networks. *Nat. Mater.* **14**, 1104–1109 (2015).
12. M. T. Barako, A. Sood, C. Zhang, J. J. Wang, T. Kodama, M. Asheghi, X. L. Zheng, P. V. Braun, K. E. Goodson, Quasi-ballistic electronic thermal conduction in metal inverse opals. *Nano Lett.* **16**, 2754–2761 (2016).
13. G. T. England, C. Russell, E. Shirman, T. Kay, N. Vogel, J. Aizenberg, The optical Janus effect: Asymmetric structural color reflection materials. *Adv. Mater.* **29**, 1606876 (2017).
14. S. Kim, A. N. Mitropoulos, J. D. Spitzberg, H. Tao, D. L. Kaplan, F. G. Omenetto, Silk inverse opals. *Nat. Photonics* **6**, 817–822 (2012).
15. M. Kolle, P. M. Salgard-Cunha, M. R. J. Scherer, F. M. Huang, P. Vukusic, S. Mahajan, J. J. Baumberg, U. Steiner, Mimicking the colourful wing scale structure of the *Papilio blumei* butterfly. *Nat. Nanotechnol.* **5**, 511–515 (2010).
16. A. R. Studart, Additive manufacturing of biologically-inspired materials. *Chem. Soc. Rev.* **45**, 359–376 (2016).
17. K. R. Phillips, G. T. England, S. Sunny, E. Shirman, T. Shirman, N. Vogel, J. Aizenberg, A colloidoscope of colloid-based porous materials and their uses. *Chem. Soc. Rev.* **45**, 281–322 (2016).
18. Y. Kang, J. J. Walsh, T. Gorishnyy, E. L. Thomas, Broad-wavelength-range chemically tunable block-copolymer photonic gels. *Nat. Mater.* **6**, 957–960 (2007).
19. D. T. Ge, E. Lee, L. L. Yang, Y. G. Cho, M. Li, D. S. Gianola, S. Yang, A robust smart window: Reversibly switching from high transparency to angle-independent structural color display. *Adv. Mater.* **27**, 2489–2495 (2015).
20. F. Fu, Z. Chen, Z. Zhao, H. Wang, L. Shang, Z. Gu, Y. Zhao, Bio-inspired self-healing structural color hydrogel. *Proc. Natl. Acad. Sci. U.S.A.* **114**, 5900–5905 (2017).
21. Y. Yue, T. Kurokawa, M. A. Haque, T. Nakajima, T. Nonoyama, X. Li, I. Kajiwara, J. P. Gong, Mechano-actuated ultrafast full-colour switching in layered photonic hydrogels. *Nat. Commun.* **5**, 4659 (2014).
22. S.-H. Kim, J.-G. Park, T. M. Choi, V. N. Manoharan, D. A. Weitz, Osmotic-pressure-controlled concentration of colloidal particles in thin-shelled capsules. *Nat. Commun.* **5**, 3068 (2014).
23. J. Ge, Y. Yin, Responsive photonic crystals. *Angew. Chem. Int. Ed.* **50**, 1492–1522 (2011).
24. H. Lee, J. Kim, H. Kim, J. Kim, S. Kwon, Colour-barcoded magnetic microparticles for multiplexed bioassays. *Nat. Mater.* **9**, 745–749 (2010).
25. J. Hou, H. Zhang, Q. Yang, M. Li, Y. Song, L. Jiang, Bio-inspired photonic-crystal microchip for fluorescent ultratrace detection. *Angew. Chem. Int. Ed.* **53**, 5791–5795 (2014).
26. M. Wang, Y. Yin, Magnetically responsive nanostructures with tunable optical properties. *J. Am. Chem. Soc.* **138**, 6315–6323 (2016).
27. H.-H. Chou, A. Nguyen, A. Chortos, J. W. F. To, C. Lu, J. Mei, T. Kurosawa, W.-G. Bae, J. B.-H. Tok, Z. Bao, A chameleon-inspired stretchable electronic skin with interactive colour changing controlled by tactile sensing. *Nat. Commun.* **6**, 8011 (2015).
28. X. Liu, T.-C. Tang, E. Tham, H. Yuk, S. Lin, T. K. Lu, X. Zhao, Stretchable living materials and devices with hydrogel–elastomer hybrids hosting programmed cells. *Proc. Natl. Acad. Sci. U.S.A.* **114**, 2200–2205 (2017).

29. Y. S. Zhang, A. Khademhosseini, Advances in engineering hydrogels. *Science* **356**, eaaf3627 (2017).
30. C. Larson, B. Peele, S. Li, S. Robinson, M. Totaro, L. Beccai, B. Mazzolai, R. Shepherd, Highly stretchable electroluminescent skin for optical signaling and tactile sensing. *Science* **351**, 1071–1074 (2016).
31. J. Teyssier, S. V. Saenko, D. van der Marel, M. C. Milinkovitch, Photonic crystals cause active colour change in chameleons. *Nat. Commun.* **6**, 6368 (2015).
32. S. R. Shin, S. M. Jung, M. Zalabany, K. Kim, P. Zorlutuna, S. B. Kim, M. Nikkhah, M. Khabiry, M. Azize, J. Kong, K.-t. Wan, T. Palacios, M. R. Dokmeci, H. Bae, X. Tang, A. Khademhosseini, Carbon-nanotube-embedded hydrogel sheets for engineering cardiac constructs and bioactuators. *ACS Nano* **7**, 2369–2380 (2013).
33. S. R. Shin, C. Shin, A. Memic, S. Shadmehr, M. Miscuglio, H. Y. Jung, S. M. Jung, H. Bae, A. Khademhosseini, X. Tang, M. R. Dokmeci, Aligned carbon nanotube-based flexible gel substrates for engineering bio-hybrid tissue actuators. *Adv. Funct. Mater.* **25**, 4486–4495 (2015).
34. L. Ricotti, T. Fujie, H. Vazão, G. Ciofani, R. Marotta, R. Brescia, C. Filippeschi, I. Corradini, M. Matteoli, V. Mattoli, L. Ferreira, A. Menciassi, Boron nitride nanotube-mediated stimulation of cell co-culture on micro-engineered hydrogels. *PLOS ONE* **8**, e71707 (2013).
35. S.-J. Park, M. Gazzola, K. S. Park, S. Park, V. D. Santo, E. L. Blevins, J. U. Lind, P. H. Campbell, S. Dauth, A. K. Capulli, F. S. Pasqualini, S. Ahn, A. Cho, H. Yuan, B. M. Maoz, R. Vijaykumar, J.-W. Choi, K. Deisseroth, G. V. Lauder, L. Mahadevan, K. K. Parker, Phototactic guidance of a tissue-engineered soft-robotic ray. *Science* **353**, 158–162 (2016).
36. F. Zheng, F. Fu, Y. Cheng, C. Wang, Y. Zhao, Z. Gu, Organ-on-a-chip systems: Microengineering to biomimic living systems. *Small* **12**, 2253–2282 (2016).
37. L. Shang, Y. Cheng, Y. Zhao, Emerging droplet microfluidics. *Chem. Rev.* **117**, 7964–8040 (2017).
38. S. N. Bhatia, D. E. Ingber, Microfluidic organs-on-chips. *Nat. Biotechnol.* **32**, 760–772 (2014).
39. A. W. Feinberg, A. Feigel, S. S. Shevkoplyas, S. Sheehy, G. M. Whitesides, K. K. Parker, Muscular thin films for building actuators and powering devices. *Science* **317**, 1366–1370 (2007).
40. P. W. Alford, A. W. Feinberg, S. P. Sheehy, K. K. Parker, Biohybrid thin films for measuring contractility in engineered cardiovascular muscle. *Biomaterials* **31**, 3613–3621 (2010).
41. L. Ricotti, B. Trimmer, A. W. Feinberg, R. Raman, K. K. Parker, R. Bashir, M. Sitti, S. Martel, P. Dario, A. Menciassi, Biohybrid actuators for robotics: A review of devices actuated by living cells. *Sci. Robot.* **2**, eaaq0495 (2017).
42. D. E. Ingber, Reverse engineering human pathophysiology with organs-on-chips. *Cell* **6**,1105–1109 (2016).
43. Y. Yu, F. Fu, L. Shang, Y. Cheng, Z. Gu, Y. Zhao, Bio-inspired helical microfibers from microfluidics. *Adv. Mater.* **29**, 1605765 (2017).
44. J. U. Lind, T. A. Busbee, A. D. Valentine, F. S. Pasqualini, H. Yuan, M. Yadid, S.-J. Park, A. Kotikian, A. P. Nesmith, P. H. Campbell, J. J. Vlassak, J. A. Lewis, K. K. Parker, Instrumented cardiac microphysiological devices via multimaterial three-dimensional printing. *Nat. Mater.* **16**, 303–308 (2016).
45. P. J. Gouveia, S. Rosa, L. Ricotti, B. Abecasis, H. V. Almeida, L. Monteiro, J. Nunes, F. S. Carvalho, M. Serra, S. Luchkin, A. L. Kholkin, P. M. Alves, P. J. Oliveira, R. Carvalho, A. Menciassi, R. P. das Neves, L. S. Ferreira, Flexible nanofilms coated with aligned piezoelectric microfibers preserve the contractility of cardiomyocytes. *Biomaterials* **139**, 213–228 (2017).
46. A. K. Schroer, M. S. Shotwell, V. Y. Sidorov, J. P. Wikswo, W. D. Merryman, I-wire heart-on-a-chip II: Biomechanical analysis of contractile, three-dimensional cardiomyocyte tissue constructs. *Acta Biomater.* **48**, 79–87 (2017).
47. G. S. Ugolini, R. Visone, D. Cruz-Moreira, A. Redaelli, M. Rasponi, Tailoring cardiac environment in microphysiological systems: An outlook on current and perspective heart-on-chip platforms. *Future Sci. OA* **3**, FSO191 (2017).

Acknowledgments

Funding: This work was supported by the National Science Foundation of China (grants 51522302 and 21473029), the NSAF Foundation of China (grant U1530260), the Fundamental Research Funds for the Central Universities, the Scientific Research Foundation of Southeast University, and the Scientific Research Foundation of Graduate School of Southeast University. **Author contributions:** Y.Z. conceived the idea and designed the experiment. F.F. carried out the experiments. F.F. and Y.Z. analyzed data and wrote the paper. L.S., Z.C., and Y.Y. assisted with experiment operations. **Competing interests:** The authors declare that they have no competing financial interests. **Data and materials availability:** All data needed to evaluate the conclusions in the paper are present in the paper and/or the Supplementary Materials. Additional data related to this paper may be requested from the authors.

Submitted 25 December 2017
Accepted 5 March 2018
Published 28 March 2018
10.1126/scirobotics.aar8580

Citation: F. Fu, L. Shang, Z. Chen, Y. Yu, Y. Zhao, Bioinspired living structural color hydrogels. *Sci. Robot.* **3**, eaar8580 (2018).

Science Robotics

Bioinspired living structural color hydrogels

Fanfan Fu, Luoran Shang, Zhuoyue Chen, Yunru Yu, and Yuanjin Zhao

Sci. Robot. **3** (16), eaar8580. DOI: 10.1126/scirobotics.aar8580

Science Robotics (ISSN 2470-9476) is published by the American Association for the Advancement of Science. 1200 New York Avenue NW, Washington, DC 20005. The title *Science Robotics* is a registered trademark of AAAS.